THE ASTROPHYSICAL JOURNAL, 333:749–753, 1988 October 15

AN IMPROVED PROPER-MOTION MEASUREMENT OF SN 1006

KNOX S. LONG[1,2] AND WILLIAM P. BLAIR[2]
Johns Hopkins University
AND
SIDNEY VAN DEN BERGH[3]
Herzberg Institute of Astrophysics, Dominion Astrophysical Observatory
Received 1988 March 14; accepted 1988 April 14

ABSTRACT

We have obtained CCD images of SN 1006 in the light of Hα, Hβ, and through a 6100 Å continuum filter in order to search for new optical filamentation and to obtain a more accurate measurement of the proper motion of the optical supernova remnant (SNR). Except for a new filament in the NW we did not find any other new emission from SN 1006 to a surface brightness limit of $\sim 5 \times 10^{-17}$ ergs cm^{-2} s^{-1} arcsec^{-2} in Hα. Here we compare the optical, radio, and X-ray data for SN 1006 and suggest a consistent overall picture for the remnant. Using our 1987 CCD image and a digitized version of van den Bergh's original plates, we infer a mean proper motion for the NW filament of 0.30 ± 0.04 arcsec yr^{-1}. This proper-motion measurement implies a distance of 1.7–3.1 kpc for SN 1006 assuming the recent determination of the shock velocity by Kirshner, Winkler, and Chevalier. We use this distance estimate to infer a maximum visual magnitude V(max) for SN 1006 intermediate to values of −6 and −9.5 suggested by Pskovskii and by Clark and Stephenson based on the historical record.

Subject headings: nebulae: individual (SN 1006) — nebulae: supernova remnants — stars: supernovae

I. INTRODUCTION

The supernova of 1006 A.D. was, like SN 1572 (Tycho), probably of Type Ia. The remnant of SN 1006 was first identified by Gardner and Milne (1965) as a limb-brightened, almost circular radio source ~30′ across. A 10′ long optical filament, discovered by van den Bergh (1976), coincides with the NW limb of the SNR. Detailed radio and X-ray images of SN 1006 are now available (Reynolds and Gilmore 1986; Roger *et al.* 1988; Pye *et al.* 1981). At radio wavelengths, the SNR is limb-brightened and exhibits bilateral symmetry, as if the SNR expansion were being constrained by a preexisting magnetic field. Bright edges are seen in the NE and SW. The X-ray image is very similar to the radio image above 1 keV although at lower energies the SNR is less limb-brightened.

The spectrum of SN 1006 at X-ray wavelengths is unusual for a limb-brightened SNR; emission lines of highly ionized S, Si, and Fe are absent. Hamilton, Sarazin, and Szymkowiak (1986) have explained the X-ray emission in terms of a thermal plasma in the reverse shock in the outer layers of the ejecta of SN 1006; the lack of line emission is due to nonionization equilibrium effects. The spectrum of SN 1006 is different because the remnant is expanding into a lower density medium than Tycho, Kepler, or Cas A. As a result, even though SN 1006 is older than these other SNRs, the S, Si, and Fe have not yet become highly ionized. The detection of weak emission from highly ionized O in soft X-rays by Vartanian, Lum, and Ku (1985) appears to support this picture. In addition, a hot OB subdwarf has been discovered which apparently lies behind the SNR (Schweizer and Middleditch 1980). UV observations of this star (hereafter the S-M star) have revealed broad (± 5000 km s^{-1}) absorption lines of Fe II, confirming the presence of large amounts of unshocked material in the SNR interior (Wu *et al.* 1983; Fesen *et al.* 1988; Hamilton and Fesen 1988).

At optical wavelengths, the spectrum of the faint NW filament is dominated by the Balmer lines of hydrogen rather than forbidden lines of cosmically abundant metals (Schweizer and Lasker 1978; Lasker 1981). Such spectra are thought to arise when a fast shock wave encounters neutral material (Chevalier and Raymond 1978; Chevalier Kirshner, and Raymond 1980; McKee and Hollenbach 1980). As a result of a charge exchange reaction between the neutrals penetrating the shock and the fast ionized hydrogen behind the shock, this model leads to the prediction of broad wings on the Balmer lines. Recently, Kirshner, Winkler, and Chevalier (1987) have detected the broad component to the Hα line in SN 1006; it has a FWHM velocity of 2600 ± 100 km s^{-1}.

In this paper we present new CCD imagery of SN 1006. The motivation for these observations was (*a*) to perform a more sensitive search of SN 1006 for additional filaments, (*b*) to compare the Hα to Hβ ratios of the filaments as a function of position, and (*c*) to obtain a more accurate measurement of the proper motion of the known filaments.

II. THE OBSERVATIONS

The observations were carried out on the 2.5 m du Pont and 1 m Swope telescopes at the Las Campanas Observatory in Chile in 1987 April, using a TI 800 × 800 CCD, a focal plane reducer, and narrow-band interference filters. The design for the focal plane reducer has been described by Gunn and Westphal (1981); the Las Campanas version is known as the CHUEI. On the du Pont telescope the plate scale was 0.41 arcsec pixel^{-1}, and the field of view was 5′.5; on the 1 m Swope

[1] Visiting Adjunct Associate, Mount Wilson and Las Campanas Observatories.
[2] Visiting Astronomer, Las Campanas Observatory, operated by the Carnegie Institution of Washington.
[3] Visiting Astronomer, Cerro Tololo Inter-American Observatory, operated by AURA, Inc., under contract to the National Science Foundation.

TABLE 1

OBSERVATION LOG OF LCO CCD IMAGES OF SN 1006

TELESCOPE	UT DATE	FIELD ID	FIELD CENTER R.A. (1950)	FIELD CENTER Decl. (1950)	FILTER	EXPOSURE (s)
1m Swope	1987 Apr 21	NW	$15^h02^m28^s.7$	−41°48′51″	Hα	3000
1m Swope	1987 Apr 21	NW	15 02 28.7	−41 48 51	6100	1000
1m Swope	1987 Apr 21	NE	15 03 43.6	−41 45 44	Hα	2000
1m Swope	1987 Apr 21	N	15 03 05.6	−41 45 45	Hα	2000
1m Swope	1987 Apr 21	N	15 03 05.6	−41 45 45	6100	800
2.5 m du Pont	1987 Apr 26	NW	15 02 14.8	−41 45 46	Hα	3000
2.5 m du Pont	1987 Apr 26	NW	15 02 14.8	−41 45 46	Hβ	3000
1m Swope	1987 Apr 27	SW	15 01 55.4	−42 01 42	Hα	2000
1m Swope	1987 Apr 27	SW	15 01 55.4	−42 01 42	6100	1000
1m Swope	1987 Apr 28	SE	15 03 38.1	−42 01 12	Hα	3000
1m Swope	1987 Apr 28	SE	15 03 38.1	−42 01 12	6100	1000

telescope the scale was 1.06 arcsec pixel^{-1}, and the field was 14′ on a side. An observing log is presented in Table 1. The characteristics of the interference filters are summarized in Table 2. As noted earlier, Kirshner, Winkler, and Chevalier (1987) have recently detected the broad component to the Hα emission in SN 1006; the broad component comprises $\sim\frac{1}{3}$ of the total emission and has a FWHM of ~ 50 Å. As a result the Hα and Hβ filters, which have FWHM of 52 and 54 Å, respectively, cut off a small portion ($< 20\%$) of the total emission from SN 1006. The images were reduced using dome flats obtained nightly through each filter and separate averaged bias frames. The images were flux-calibrated using standard stars—principally LTT 6248—from the list of Stone and Baldwin (1983). However, the observing conditions were not photometric for most exposures. We have attempted to use stars from the Hubble Space Telescope guide star catalog for this region to partially compensate for varying conditions, but the flux estimates are still fairly coarse ($\pm 30\%$). All of the reductions were carried out using IRAF at Johns Hopkins.

Only one SN 1006 field was observed with the 2.5 m du Pont telescope. This field contains the crispest filaments in van den Bergh's (1976) optical discovery photographs of SN 1006, The resulting Hα image, obtained by averaging the three individual exposures, is shown in Figure 1 (Plate 20). Individual stars have FWHM of $\sim 1''$ in this image. The wavy veil-like character of the emission is typical of the Balmer-dominated filaments observed in other SNRs such as Tycho's SNR and DEM 71 in the Large Magellanic Cloud (LMC). The width of the filament is 8″–10″, $\sim 1/60$ of the length, 1/90 of the radius of the SNR. The dynamic range in the brightest filaments is about a factor of 10; the brightest portions have a surface brightness of $\sim 5 \times 10^{-16}$ ergs cm^{-2} s^{-1} arcsec^{-2} in Hα. We estimate the faintest stars in Figure 1 to be $m_{6575} \sim 22$, based on the count rate for stars in common with the Hubble Space Telescope guide star catalog for this region. Although the image is qualitatively similar to van den Bergh's photograph, the signal-to-noise ratio is higher and a bubble-like filament can be observed $\sim 1'$ ahead of the brighter filaments. This filament is located on the faint, outermost radio contours in the VLA map of Reynolds and Gilmore (1986).

TABLE 2

FILTER CHARACTERISTICS

Name	λ_c (Å)	$\Delta\lambda$ (FWHM [Å])	T_{peak}
Hα	6575	52	62%
Hβ	4866	54	68
Continuum	6100	150	65

The Hβ image of this region is almost identical to the Hα image. There are no significant differences in the Hα/Hβ ratio anywhere along the bright portion of the filament. The observed flux ratio is consistent with the value of 3–4 which has been observed spectroscopically by Lasker (1981), but is not consistent with a ratio of 6–8 which had been reported earlier (Schweizer and Lasker 1978).

On the Swope telescope, we obtained images of most of the remainder of the radio/X-ray SNR (see Table 1). As anticipated, the sensitivity to diffuse emission is approximately the same for the two telescopes and we easily detected the previously known filaments through our ~ 50 Å wide Hα filter. Figure 2 (Plate 21), a mosaic of data from the NW and N fields shows the entire Hα filament along the NW limb of SN 1006; the new emission outside the main filament is also visible. The faintest stars in the image have $m_{6575} \sim 20$. Because of telescope collimation problems, the imaging properties of the CHUEI on the Swope telescope were not ideal: (*a*) We were unable to focus the image over the entire surface of the detector; as a result the effective seeing ranged from about 2″ at the center to 4″ at the edge of the 14′ field. (*b*) There are occasional ghosts of bright stars in the images; one is apparent near the center of Figure 2. Also, very bright stars can cause internal reflections that show as arcs; one of these is visible in Figure 2. These features are easy to distinguish from filaments, however, since they are visible in both the continuum and Hα exposures. (*c*) Finally, there was a scattering problem along the western edge of the images. Despite these "cosmetic" defects, the images show much more detail than van den Bergh's discovery plates. All of the images have been searched for new optical emission from SN 1006. None was detected to a surface brightness limit a factor of ~ 10 below that of the bright filament in the NW. Evidently, if there are any additional optical filaments around the rest of the shell, it will take a very determined search to detect them.

III. PROPER MOTION OF THE NW FILAMENT

Hesser and van den Bergh (1981) have measured the proper motion of the NW filament previously. Based on a comparison of the 1976 discovery plates and CTIO 4 m direct plates taken in 1981, they reported a mean proper motion of the NW filament of 0.39 ± 0.06 arcsec yr^{-1} from measurements at 11 posi-

PLATE 20

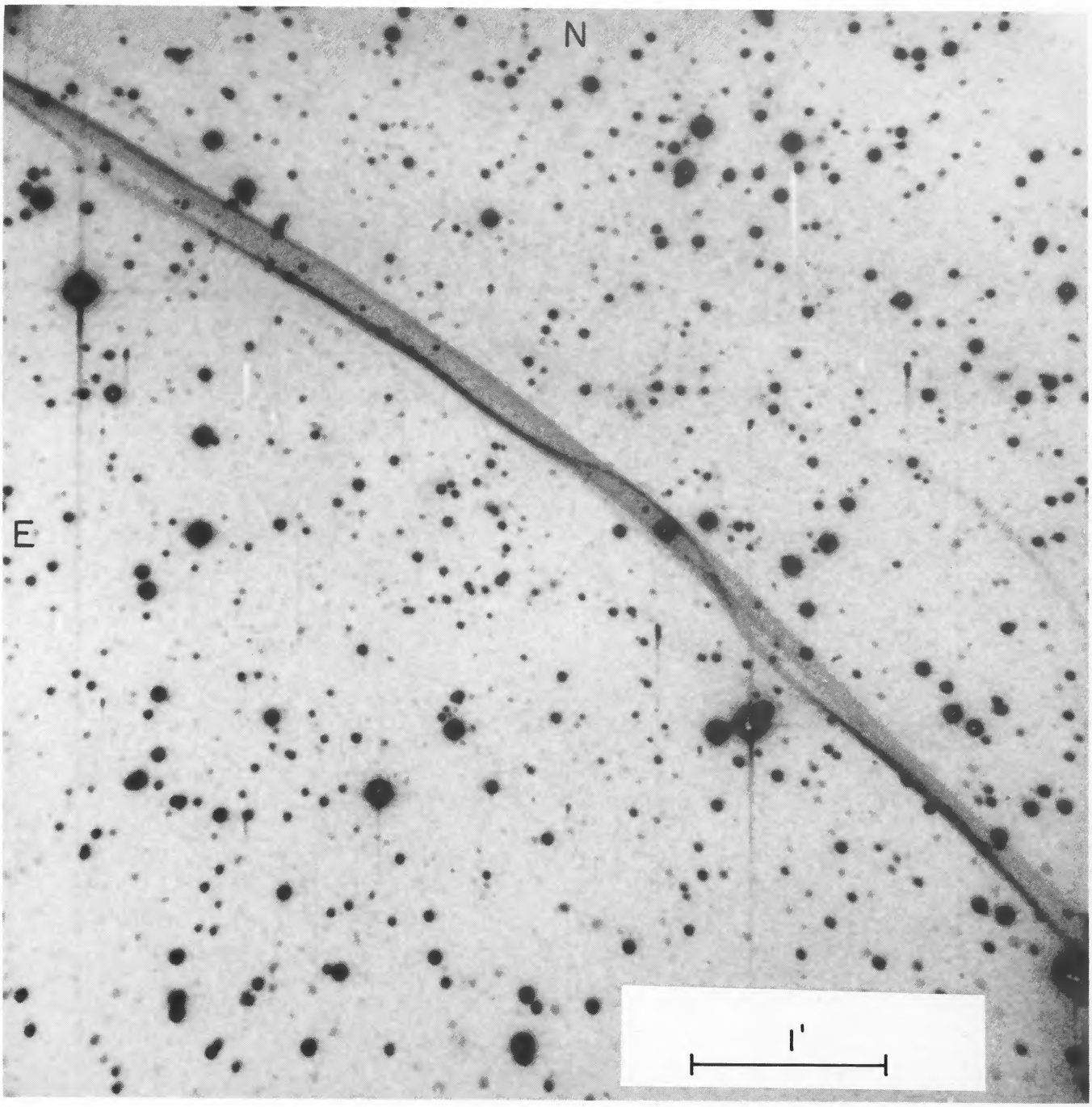

FIG. 1.—Deep 3000 s Hα image of a portion of the NW filament of SN 1006 obtained with the 2.5 m du Pont telescope using the CHEUI as a focal plane reducer. The field is 5'.5 on a side. North is up, and east to the left. Note the faint filament ~1' NW of the western end of the bright filament.

LONG, BLAIR, AND VAN DEN BERGH (*see* **333**, 750)

1988ApJ...333..749L

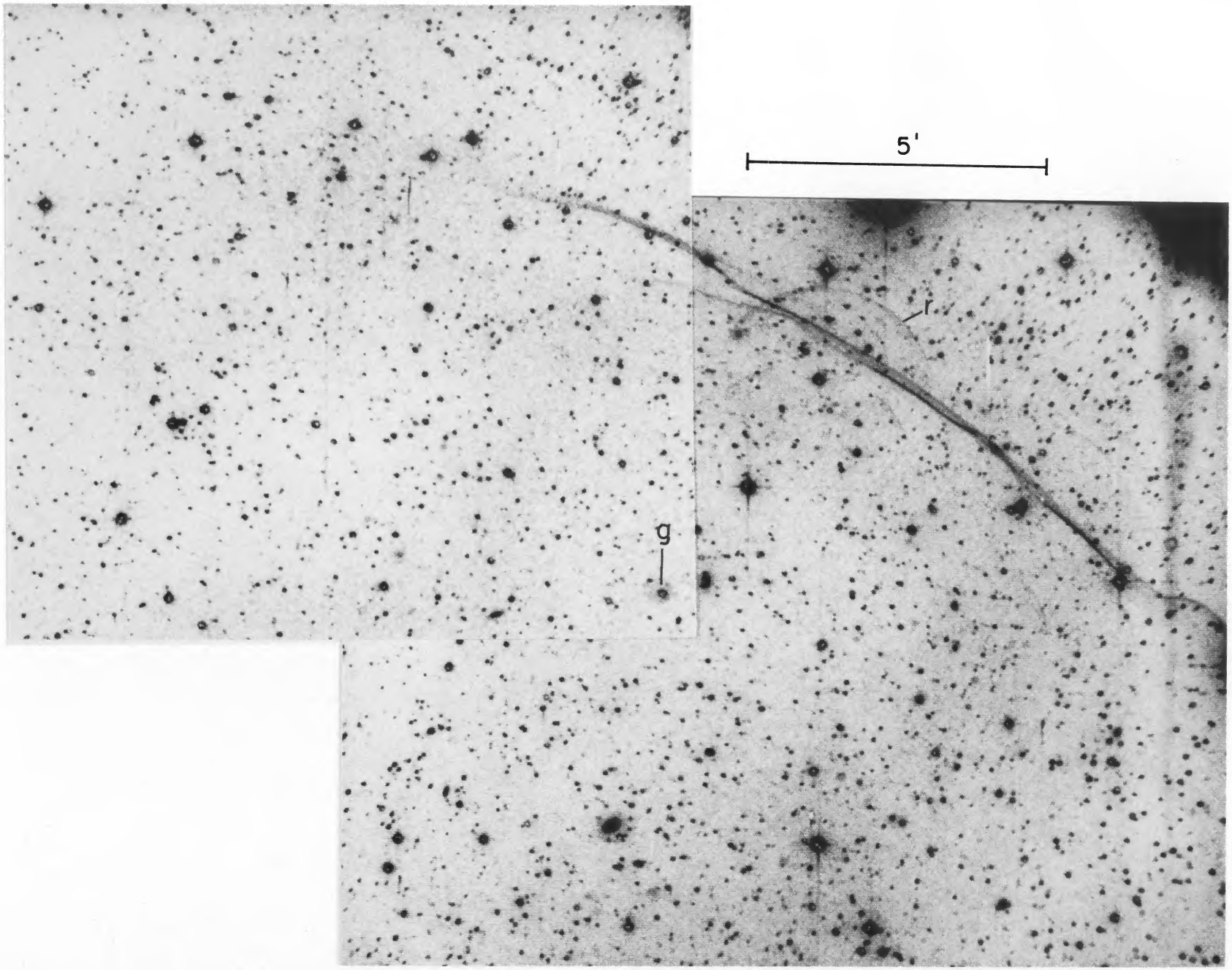

FIG. 2.—Mosaic comprised of portions of two CCD frames showing nearly all of the NW filament of SN 1006. The semicircular shaped feature, indicated by the "r" on the picture, is a reflection of from a bright star and is visible in the continuum image as well. The feature marked "g" is also a stellar ghost image.

1988ApJ...333..749L

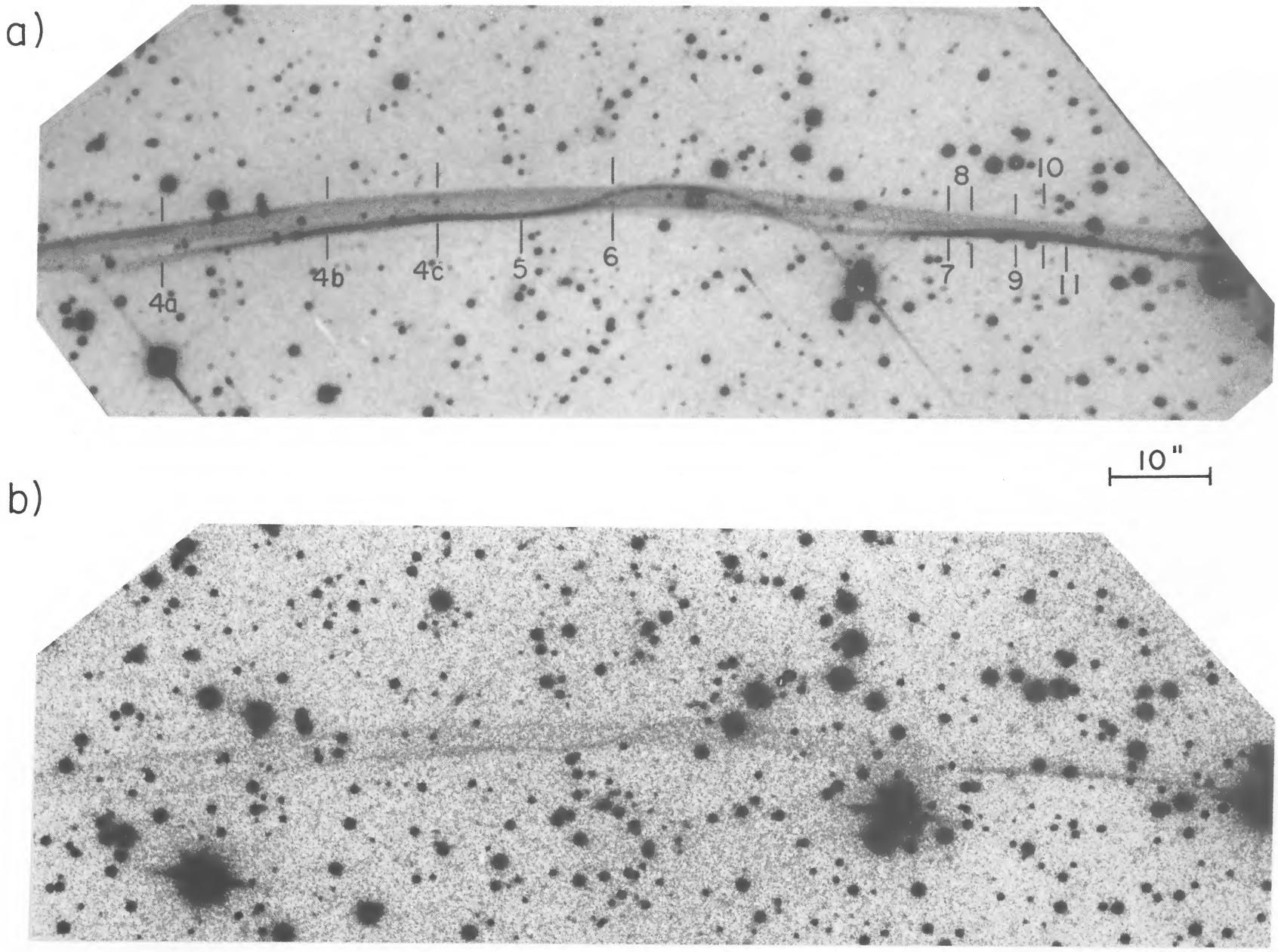

FIG. 3.—Comparison of (*a*) our 1987 CCD image of SN 1006 and (*b*) one of van den Bergh's (1976) original discovery photographs. Positions at which we measured the proper motion are indicated on the upper panel.

TABLE 3

PROPER-MOTION MEASUREMENTS

Position	Proper Motion (arcsec yr^{-1})
4	0.33
4[b]	0.33
4[c]	0.30
5	0.31
6	0.33
7	0.30
8	0.33
9	0.22
10	0.26
11	0.26

NOTE.—The letters "b" and "c" indicate we have measured additional locations along the filament (in excess of those used in a previous paper by other authors. "b" and "c" are between positions 4 and 5 in the earlier paper.)

tions. They also reported considerable scatter in the measurements for various portions of the filament, ranging from 0.14 to 0.85 arcsec yr^{-1}.

In an attempt to improve upon the original measurements, we have compared the Hα image in Figure 1 to the original 1976 plates. As shown in Figure 3 (Plate 22), the proper motion of the filaments over an 11 yr baseline is very evident. On the other hand, allowing for the different sensitivities of the two images there are no obvious changes in the morphology of the filament, despite the fact that the filament has moved $\sim\frac{1}{2}$ of its width.

To determine the proper motion, we had portions of the original 1976 plates (P1980 and P2014) digitized in 20 μm (=0".37) steps using the PDS machine at NASA/GSFC. Using IRAF, we geometrically transformed and rescaled the PDSed images, and registered them with the CCD Hα image to an accuracy of less than or equal to 0".4 (1 pixel). We then rotated both the CCD and the digitized images so that the filament was oriented along one of the principal axes of the array. It was then straightforward (and as accurate as any other method with which we experimented) to measure the position of the filament in the two images using a cursor on an image display system. (In all cases, we checked that the image was registered locally using stars near the filament position.) Repeated measurements are accurate to $\sim$1 pixel, which corresponds to an error of $\pm$0.037 arcsec yr^{-1}. Results of the individual measurements are shown in Table 3; locations of the measurements are shown in Figure 3. Wherever possible, we have attempted to use the same positions used by Hesser and van den Bergh (1981). We find a mean proper motion for the NW filament of 0.30 ± 0.04 arcsec yr^{-1}. In addition, the expansion is much more uniform than was reported by Hesser and van den Bergh (1981), varying only from 0.22 to 0.33 arcsec yr^{-1}.

Our measurement is an improvement over that reported by Hesser and van den Bergh (1981) for a number of reasons. The time baseline for this measurement is longer by more than a factor of 2. Also, our second epoch image is much deeper than any of the photographic images permiting a less ambiguous identification of features. The magnitude of the apparent position-to-position variation in the expansion velocity reported by Hesser and van den Bergh is almost surely due to measurement uncertainties (a possibility that they did not include), which were largely due to the fact that their second epoch plate was obtained in rather poor seeing.

IV. DISCUSSION

Based on a shock velocity estimate of 2800–3870 km s^{-1} inferred from an analysis of the broad wings in the Hα profile of SN 1006 and the earlier determination of the proper motion, Kirshner, Winkler, and Chevalier (1987) derived a distance of 1.5–2.1 kpc for SN 1006. Using our improved determination of 0.30 arcsec yr^{-1} for the proper motion leads to a revised estimate of 2.1–2.7 kpc for SN 1006. (Including the uncertainty in the proper motion, the full range of allowed distances increases to 1.7–3.1 kpc) Using Fesen *et al.*'s (1988) revised distance estimate for the S-M star (1.5–3.3 kpc), it is still possible to have the S-M star behind the SNR as it must be (see Fesen *et al.* 1988).

The immediate ramifications of this larger distance estimate are apparent from inspection of the summary given in Table 4. The extremes are given by the largest allowed proper motion with the smaller velocity estimate and the smallest proper motion with the larger velocity estimate. For the permitted distance range, the SNR diameter is $\sim$16–28 pc (assuming an average angular diameter of 31′ from Reynolds and Gilmore 1986) and the Z distance is $\sim$450–800 pc. Most surprising, however, is the mean expansion velocity required which should be in the range $\sim$8000–14,000 km s^{-1}. The homogeneity of the SN Ia expansion velocities is still actively debated (Branch 1987; Pearce, Colgate, and Petschek 1988), but most Type Ia SNe show a fairly uniform peak expansion velocity. For instance, Branch (1977) found $V_{SN} = 10{,}900 \pm 700$ km s^{-1}

TABLE 4

RANGE OF ALLOWED VALUES

	Velocity			
	2800 km s^{-1}		3870 km s^{-1}	
Parameter	0".26 yr^{-1}	0".34 yr^{-1}	0".26 yr^{-1}	0".34 yr^{-1}
Distance (kpc)	2.3	1.7	3.1	2.4
Diameter (pc)	20.5	15.7	28.3	21.6
Z (pc)	570	440	790	600
$\langle V_{exp} \rangle$ (km s^{-1})	10200	7800	14100	10800
Swept-up mass ($M_\odot$) (per $n_0 = 0.01$ cm^{-3})	1.10	0.49	2.89	1.29

1988ApJ...333..749L

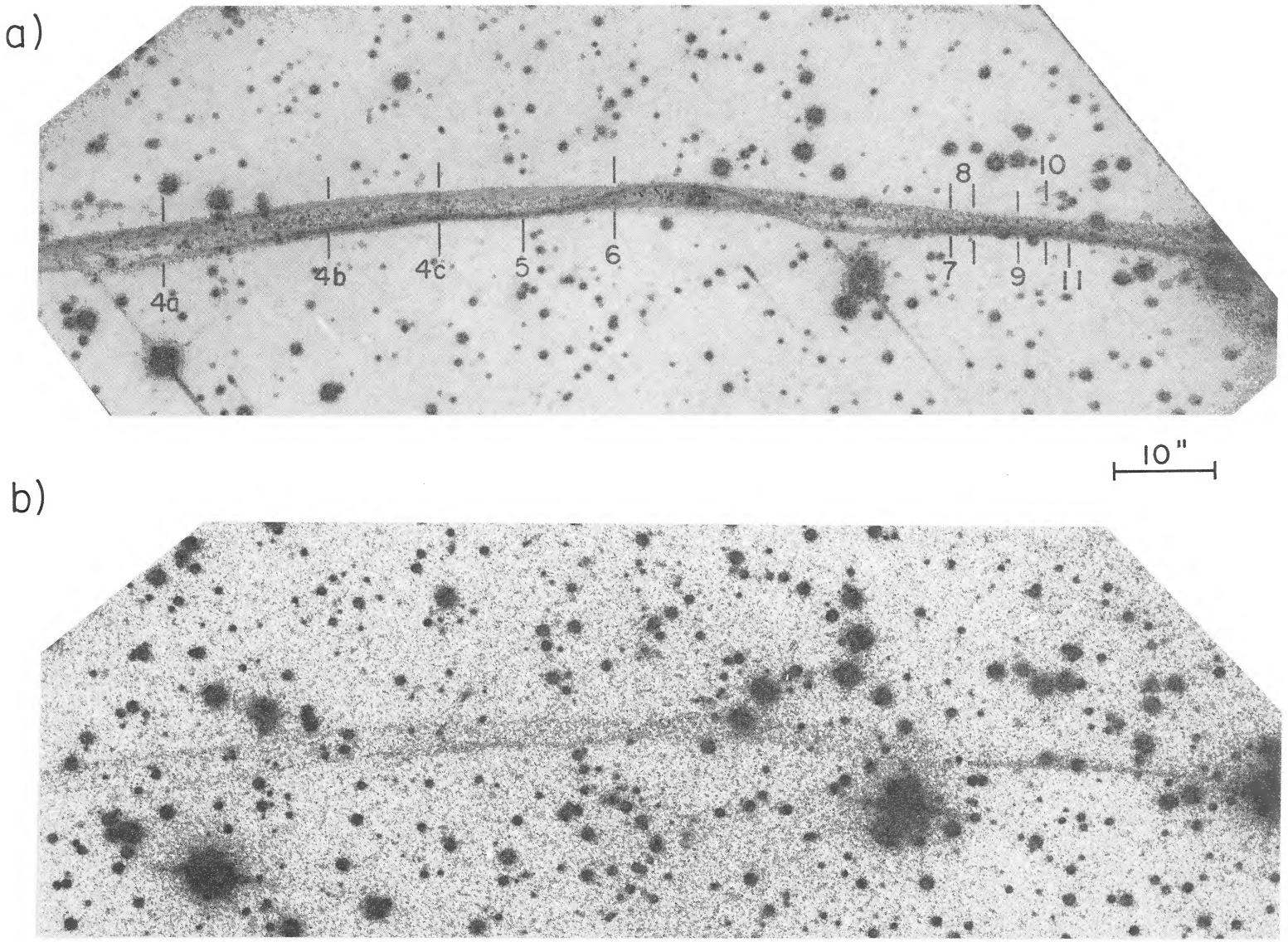

FIG. 3.—Comparison of (*a*) our 1987 CCD image of SN 1006 and (*b*) one of van den Bergh's (1976) original discovery photographs. Positions at which we measured the proper motion are indicated on the upper panel.

from a study of 11 Type I Sne. If SN 1006 was a Type Ia (and recent models and observations indicate that it was—see Hamilton and Fesen [1988] and references therein) and if it did not have an abnormally high peak ejection velocity, the high mean expansion velocity derived above implies very little deceleration has taken place in SN 1006. By way of comparison, the mean expansion velocity for SN 1572 is only ~ 6000 km s^{-1} (Chevalier, Kirshner, and Raymond 1980). Since a reverse shock in the outer layers of ejecta appears necessary to explain the SNR's X-ray emission (Hamilton, Sarazin, and Szymkowiak 1986), some deceleration must have taken place. Again assuming a normal initial Type I expansion velocity, this argues for a distance toward the lower end of the permitted range, say less than or equal to 2.4 kpc. We note that for the typical preshock densities of 0.05–0.07 cm^{-3} inferred for the interstellar medium (ISM) surrounding SN 1006 (cf. Hamilton and Fesen 1988), the swept-up mass should be of order 3-10 $M_\odot$ (i.e., several times the expected ejecta mass from a Type I carbon deflagration model such as W7 of Nomoto, Thielemann, and Yokoi 1984). This is consistent with the relatively recent formation of a reverse shock in SN 1006 (perhaps indicated by the power-law X-ray spectrum in SN 1006 as opposed to the thermal line emission seen in SN 1572).

The apparent magnitude of SN 1006 at maximum light remains controversial. According to Cadonau, Sandage, and Tammann (1985) the supernovae of Type I in elliptical galaxies (i.e., SN Ia) yield $M_B \approx M_V = -18.2 + \log H_0/100$. From galaxy counts and H I observations, Burstein and Heiles (1982) estimate $E_{B-V} = 0.09$ in the direction of SN 1006 from which we obtain $A_V = 0.28$. If SN 1006 were typical, then our distance limits can be used to estimate the apparent magnitude at maximum. Specifically, $-6.8 < V(\max) < -5.4$ for $H_0 = 100$ or $-8.3 < V(\max) < -7.0$ for $H_0 = 50$. Estimates of $V(\max)$ based on the historical record range from -9.5 (Clark and Stephenson 1977) to -6 ± 0.5 (Pskovskii 1978). Our results are consistent with either of the previous estimates depending upon H_0, but tend to favor a $V(\max)$ somewhat fainter than estimated by Clark and Stephenson.

Rationalizing the presence of the optical Balmer filaments only along the NW limb of the SNR where the X-ray/radio shell is weakest is not straightforward. The sharpness of the filament coupled with the existence of broad and narrow Balmer emission implies we must be observing the primary shock front at a point where it is encountering (at least partially) neutral material; it also implies a viewing geometry very nearly edge-on. The smoothness and relative uniformity along the shock suggests that the ISM in the NW is quite uniform. As discussed by Reynolds and Gilmore (1986) the bright optical filaments in SN 1006 lie outside the brightest radio contours in the NE but inside the outermost contours. This is most likely a projection effect; there is no reason to believe there is radio emission outside the shock front as delineated by the Balmer emission. In fact, the new faint filament we found in the NW is at the edge of the radio emission. If our theoretical understanding of the Balmer filaments is correct, then the lifetime of a neutral particle penetrating the shock is short (a few years) consistent with the narrowest filaments seen ($<2''$). The difference in the position and thickness of the radio shell in the NW could either be due to a longer time scale to generate fields and high-energy electrons or due to the displacement of the contact interface between the shock-heated ISM and the ejecta from the primary shock. The angular distance between the optical filaments and the peak of the radio emission in the NW is $\sim 30''$, which corresponds to a time period of ~ 100 yr at the present expansion rate of the filaments.

Although our search for optical emission was more sensitive than previous surveys of SN 1006, we found no new emission ($\geq 5 \times 10^{-17}$ ergs cm^{-2} s^{-1} arcsec^{-2}) except for one filament in the NW. Visible absorption along the line of sight to SN 1006 is small ($A_V \sim 0.28$) and variations in the absorption are unlikely to account for the lack of observed emission in the other quadrants. Projection effects are clearly important in determining what we see since the optical shell is so thin, but nevertheless should tend to produce a general correspondence of X-ray/radio and optical surface brightness. This is the case in other young SNRs with Balmer-dominated optical emission. But in SN 1006, the bright portions of the X-ray and radio shell are in the NE and SW.

A simple explanation for the optical morphology is that while most of the SNR is encountering ionized material, the NW portion of the SNR is encountering some neutral material. In the shock responsible for Balmer-dominated filaments, each neutral hydrogen atom produces a fixed number of Balmer photons as it is ionized and as a result the surface brightness is proportional to n rather than n^2. As a result the density of ionized material in the NW must be ~ 10 times greater in the NW than elsewhere (leaving questions of geometry aside). If the total density of material is greater in the NW then one would expect the radius to be smaller in the region exhibiting optical emission, which is indeed the case. Furthermore, if the shock was encountering a mostly neutral interstellar cloud in the NW in pressure equilibrium with mostly ionized intercloud material elsewhere, then the density and ionization differences could easily account for the lack of Balmer emission except in the NW.

In this picture, however, the weakness of the X-ray emission along the NW edge of the SNR is difficult to understand. Although X-ray emission in SN 1006 is thought to arise for the most part from shocked ejecta rather than shocked ISM, it would be surprising for the portion of the shock encountering the densest ISM to be faintest in X-rays. (By way of contrast, Balmer emission in Tycho's SNR correlates fairly well with X-ray and radio emission.) Pye *et al.* (1981) note that differences in X-ray absorption along the line of sight could in principle account for the fainter X-ray emission in the NW of SN 1006. However, the X-ray and radio morphologies of SN 1006 are very similar and the radio emission is not affected by absorption. As a result it seems unlikely that the X-ray morphology is due to absorption.

Roger *et al.* (1988) have pointed out the striking bilateral symmetry of SN 1006 about an axis that runs roughly from NW to SE and argue that it is due to modification of the shock wave by the preexisting magnetic field. By analogy to interplanetary and laboratory shocks, they argue that shock propagation along the field lines (i.e., along the axis) is relatively inefficient at heating the gas to X-ray temperatures and accelerating electrons to relativistic energies.[4] Thus the shocks to the NW and SE in SN 1006 would not be able to produce strong X-ray or radio emission, which agrees with observations. If particle acceleration is more efficient for shock propa-

[4] Note that Roger *et al.* contend that shock propagation along field lines lacks a "clear discontinuity," which agrees with the appearance of the remnant in radio and X-rays. However, the crispness of the optical Balmer filaments argues for a sharp shock front at this position in SN 1006.

gation mainly perpendicular to the ambient field, then ionization could proceed more rapidly at these locations and as a result the X-ray emissivity can be higher there even though the density is the same or lower. Possibly, the strong X-ray/UV emission can even be responsible for preionizing the ISM ahead of the shock in the NE and SW, eliminating the preconditions for Balmer filaments at these locations.

We wish to thank the Mount Wilson and Las Campanas Observatories of the Carnegie Institution of Washington for the use and support of the telescopes and intrumentation necessary to carry out these observations. We would also like to thank Bob Cornett for his help in carrying out the digitization of the 1976 images of SN 1006 using the PDS machine at NASA/GSFC. We appreciate the help of Conrad Sturch and his associates at STScI for making the HST guide star data for the SN 1006 region available to us. One of us (S. v. d. B) thanks Victor Blanco for his kind hospitality at CTIO. This work was supported by the Center for Astrophysical Sciences of the Johns Hopkins University.

REFERENCES

Branch, D. 1977, *M.N.R.A.S.*, **179**, 401.
———. 1987, *Ap. J. (Letters)*, **316**, L81.
Burstein, D., and Heiles, C. 1982, *A.J.*, **87**, 1165.
Cadonau, R., Sandage, A., and Tammann, G. A. 1985, in *Supernovae as Distance Indicators*, ed. N. Bartel (Berlin: Springer), p. 151.
Chevalier, R. A., Kirshner, R. P., and Raymond, J. C. 1980, *Ap. J.*, **235**, 186.
Chevalier, R. A., and Raymond, J. C. 1978, *Ap. J. (Letters)*, **225**, L27.
Clark, D. H., and Stephenson, F. R. 1977, *The Historical Supernovae* (Oxford: Pergamon), p. 135.
Fesen, R. A., Wu, C.-C., Leventhal, M., and Hamilton, A. J. S. 1988, *Ap. J.*, **327**, 164.
Gardner, F. F., and Milne, D. K. 1965, *A.J.*, **70**, 754.
Gunn, J. E., and Westphal, J. A. 1981, *Proc. SPIE*, **290**, 16.
Hamilton, A. J. S., and Fesen, R. A. 1988, *Ap. J.*, **327**, 178.
Hamilton, A. J. S., Sarazin, C. L., and Szymkowiak, A. E. 1986, *Ap. J.*, **300**, 698.
Hesser, J. E., and van den Bergh, S. 1981, *Ap. J.*, **251**, 549.
Kirshner, R. P., Winkler, P. F., and Chevalier, R. A. 1987, *Ap. J. (Letters)*, **315**, L135.
Lasker, B. M. 1981, *Ap. J.*, **244**, 517.
McKee, C. F., and Hollenbach, D. J. 1980, *Ann. Rev. Astr. Ap.*, **18**, 219.
Nomoto, K., Thielemann, F.-K., and Yokoi, K. 1984, *Ap. J.*, **286**, 644.
Pearce, E. C., Colgate, S. A., and Petschek, A. J. 1988, *Ap. J. (Letters)*, **325**, L33.
Pskovskii, Y. P. 1978, *Soviet Astr.*, **22**, 420.
Pye, J. P., Pounds, K. A., Rolf, D. P., Seward, F. D., Smith, A., and Willingale, R. 1981, *M.N.R.A.S.*, **194**, 569.
Reynolds, S. P., and Gilmore, D. M. 1986, *A.J.*, **92**, 1138.
Roger, R. S., Milne, D. K., Kesteven, M. J., Wellington, K. J., and Haynes, R. F. 1988, *Ap. J.*, **332**, 940.
Schweizer, F., and Lasker, B. M. 1978, *Ap. J.*, **226**, 167.
Schweizer, F., and Middleditch, J. 1980, *Ap. J.*, **241**, 1039.
Stone, R. P. S., and Baldwin, J. A. 1983, *M.N.R.A.S.*, **204**, 347.
van den Bergh, S. 1976, *Ap. J. (Letters)*, **208**, L17.
Vartanian, M. H., Lum, K. S. K., and Ku, W. H.-M. 1985, *Ap. J. (Letters)*, **288**, L5.
Wu, C.-C., Leventhal, M., Sarazin, C. L., and Gull, T. R. 1983, *Ap. J. (Letters)*, **269**, L5.

WILLIAM P. BLAIR and KNOX S. LONG: Department of Physics and Astronomy, 170 Rowland Hall, Johns Hopkins Univesity, Baltimore, MD 21218

SIDNEY VAN DEN BERGH: Herzberg Institute/National Research Council, Dominion Astrophysical Observatory, 5071 W. Saanich Road, Victoria, BC V8X 4M6, Canada